Plasma Chem Plasma Process (2008) 28:107–122
DOI 10.1007/s11090-007-9113-z

ORIGINAL PAPER

Thermophysical Properties of H_2O–Ar Plasmas at Temperatures 400–50,000 K and Pressure 0.1 MPa

Petr Křenek

Received: 15 May 2007 / Accepted: 16 November 2007 / Published online: 29 November 2007

Abstract The article presents the calculation of thermophysical properties of the mixture water steam–argon which has been used to further enhance the characteristics of plasma torches stabilized by the water wortex. The calculations were performed at the temperatures 400–50,000 K and at 0.1 MPa. First, the composition and thermodynamic properties are determined by classical methods. Further the calculations of viscosity, electrical conductivity and thermal conductivity of the mixture are computed in the 4th approximation of the Chapman–Enskog method. The computation of collision integrals is described with special respect to the interactions of charged particles where the necessary calculations for the Coulomb potential screened at the Debye length were enlarged to cover the 4th approximation. Then the formulae describing the method based on the variational principle of solving the system of Boltzmann integrodifferential equations are shortly introduced and the transport coefficients are presented.

Keywords Thermophysical properties of thermal plasmas · Ionized gas mixtures · Plasma composition · Thermodynamic properties · Lennard–Jones interaction potential · Screened Coulomb potential · Effective collision cross sections · Collision integrals · Chapman–Enskog method in the 4th approximation · Viscosity · Electrical conductivity · Thermal conductivity

Nomenclature

T	Temperature
p	Total pressure
n	Total particle density
k	Boltzmann constant
R	Molar gas constant
e	Electron charge
m_e	electron mass
h	Planck constant

P. Křenek (✉)
Institute of Plasma Physics AS CR, Prague, Czech Republic
e-mail: krenek@ipp.cas.cz

ε_o	Dielectric constant
Q_i	Internal partition function of the monatomic individual species i
E_{ij}	j-th energy level of the monatomic individual species i
g_{ij}	Statistical weight of the j-th energy level E_{ij}
E_{iI}	Ionization energy of the monatomic individual species i
δE_I	Ionization energy lowering
λ_D	Debye shielding length
n_k	Particle density of k-th component
z_k	Charge of k-th component
H_i^o	Standard-state enthalpy of the monatomic individual species i
c_{pi}^o	Standard-state heat capacity of the monatomic individual species i
S_i^o	Standard-state entropy of the monatomic individual species i
M_i	Molar mass of the monatomic individual species i
Q_{ip}, Q_{ipp}	Auxiliary quantites related to the 1st and 2nd derivatives of Q_i
$K_{A_{(N+1)+}}$	Equilibrium constant of the ionization of N-times ionized monatomic species A
$Q_{A_{N+}}$	Internal partition function of N-times ionized monatomic species A
$Q_{A_{(N+1)+}}$	Internal partition function of $N + 1$-times ionized monatomic species A
$E_{A_{N+}}$	ionization energy of N-times ionized monatomic species A
q	Molar amount of argon in the mixture
x_i	Molar fraction of i-th component
m_i	Particle mass of i-th component
ps	Number of components
ρ	Equilibrium mass density of the mixture
H	Equilibrium enthalpy of the mixture
M	Molar mass of the mixture
S	Equilibrium entropy of the mixture
c_p	Equilibrium heat capacity of the mixture at constant pressure
c_v	Equilibrium heat capacity of the mixture at constant volume
a	Equilibrium sound velocity
$T\alpha_p$	Isobaric thermal expansion
$p\beta_T$	Isothermal compressibility
η	Viscosity [kg/m/s]
σ	Electrical conductivity [A/V/m]
D_{ij}	Diffusion coefficient of component i into component j
D_i^T	Coefficient of thermal diffusion of component i
λ'	Translational thermal conductivity including electron component
λ_t	Thermal diffusion component of translational thermal conductivity
a_{im},b_{im}, c_{im}^{ji}	Solutions of the system of Boltzmann equations
$Q_{ij}^{(m,m')}$	Coefficients in the system of Boltzmann equations
δ_{ik}	Cronecker delta
ζ	Order of the Enskog–Chapman approximation
$M_{mm'}^l, N_{mm'}^l$	Matrix elements of the linearized Boltzmann collision operator
μ, μ_k	Reduced mass
λ_{int}	Internal thermal conductivity
λ_{re}	Reaction thermal conductivity
Hr_i	Enthalpy of reaction constituting the i-th complex component
q_{ij}	Effective collision cross section between particles i and j

sk_{ij}	Stoichiometric coefficient
$\Omega_{ij}^{(s,r)}$	Collision integral
$\Omega^{(s,r)*}$	Reduced (dimensionless) collision integral
γ	Dimensionless velocity
T^*	Reduced temperature
r_{ij}	Particle diameter
σ_{LJ}, $(\varepsilon/k)_{LJ}$	Lennard–Jones (6–12) parameters
ξ $[A^3]$	Polarizability of neutral particle

Introduction

Plasma torches stabilized by water vortex are frequently used for plasma spraying and for waste and biomass gasification [1]. The main advantages are very high plasma enthalpy and temperature and low plasma mass flow rate which means high spraying rates and high melting points in plasma spraying and high efficiency and good control of composition of gases in plasma gasification. For this purpose, the thermophysical properties of water plasmas were studied extensively [2]. The hybrid argon–water stabilized torch [3] combines the advantages of both water vortex and gas flow stabilization systems thank special thermophysical properties of argon. The article presents detailed calculations of properties of plasma created by mixture of argon with water steam. The effect of argon molar amount ratio on basic high temperature gas mixture properties will be discussed.

The water–argon mixture can be described by the formula $(H_2O)_{(1-q)}Ar_q$ where the argon molar amounts q were chosen from 0 to 1 step 0.1. In the present paper we report calculations of the thermodynamic properties and the transport coefficients of this gas mixture according to the Chapman–Enskog method in the 4th approximation described e.g. in [4]. To take into account high efficiency and with respect to the technical potential of hybrid water-argon plasma torch performance the temperature range has been chosen from 400 to 50,000 K. The pressure 0.1 MPa of interest has been the atmospheric expansion. The plasma is supposed to be sufficiently near to the local thermodynamic equilibrium.

Although the atomic and molecular data to cover the dissociation temperature region are sufficiently accessible and frequently discussed, the high temperature region goes far beyond standard thermochemical tables and brings about the presence of multiply charged ions. On one side it means advantage by utilization of generally accessible atomic energy levels, on the other it is necessary to assure the convergence of Sonine polynomial series in almost fully ionized gas mixture by screening the Coulomb potential.

Composition and Thermodynamic Properties

In the mixture $(H_2O)_{(1-q)}Ar_q$ we supposed following decomposition products: e, H, O, Ar, O^+, O^{2+}, O^{3+}, O^{4+}, O^{5+}, O^{6+}, O^-, O_2, O_2^+, O_2^-, O_3, H^+, H^-, H_2, H_2^+, H_3^+, OH, OH^+, OH^-, HO_2, HO_2^-, H_2O, H_2O^+, H_3O^+, H_2O_2, Ar^+, Ar^{2+}, Ar^{3+}, Ar^{4+}, Ar^{5+}, Ar^{6+}. The values of enthalpy, entropy, specific heat and equilibrium constants of individual components are up to 20,000 K available in commonly accepted tables [5, 6]. For higher temperatures and especially for multiply charged ions it was necessary to perform calculations of internal partition functions for components H, O, Ar, O^+, O^{2+}, O^{3+}, O^{4+}, O^{5+}, O^{6+}, H^+, Ar^+, Ar^{2+}, Ar^{3+}, Ar^{4+}, Ar^{5+}, Ar^{6+} which can be treated as ideal monatomic gases where the internal

partition function of i-th component can be calculated taking the energy levels E_{ij} and the statistical weights g_{ij} e.g. from [7].

$$Q_i = \sum_j g_{ij} \exp\left(-\frac{E_{ij}}{kT}\right) \tag{1}$$

where $E_{ij} \leq E_{iI} - \delta E_I$, E_{iI} being the ionization energy and δE_I the ionization potential lowering

$$\delta E_I = \frac{e^2}{4\pi\varepsilon_0 \lambda_D} \tag{2}$$

with

$$\lambda_D^2 = \frac{\varepsilon_0 kT}{e^2 \sum_k z_k^2 n_k}. \tag{3}$$

It is clear that δE_I can be determined after the composition is calculated. In this work only two iterations were used which gives satisfactory results.

After having δE_I we can not only calculate values Q_i for monatomic species mentioned but also the values of their individual enthalpies (see e.g. [5, 6, 8]).

$$H_i^0(T) - H_i^0(0) = RT\left(2.5 + \frac{Q_{ip}}{Q_i}\right) \tag{4}$$

its specific heats

$$c_{pi}^0(T) = R\left[2.5 + \frac{Q_{ipp}}{Q_i} - \left(\frac{Q_{ip}}{Q_i}\right)^2\right] \tag{5}$$

and entropies

$$S_i^0(T) = R\left(2.5 \ln T + 1.5 \ln M_i - 1.16487 + \ln Q_i + \frac{Q_{ip}}{Q_i}\right) \tag{6}$$

where

$$Q_{ip} = \sum_j \frac{E_{ij}}{kT} \exp\left(-\frac{E_{ij}}{kT}\right); \quad Q_{ipp} = \sum_j \left(\frac{E_{ij}}{kT}\right)^2 \exp\left(-\frac{E_{ij}}{kT}\right).$$

Further the equilibrium constants for an ionization reaction of N-times ionized species A can be computed

$$K_{A_{(N+1)+}} = \frac{p}{kT} \cdot \left(\frac{h^2}{2\pi m_e kT}\right)^{3/2} \cdot \frac{Q_{A_{N+}}}{2Q_{A_{(N+1)+}}} \cdot \exp\left(\frac{E_{A_{N+}}}{kT}\right) \tag{7}$$

where the ionization potentials $V_{A_{N+}}$ or H, O and Ar atoms and its ions up to 5+ were also taken from the mentioned NIST Atomic Spectra Database [7].

The composition of the water–argon plasma has been defined as a stoichiometric combination of molar amounts $(H_2O)_{(1-q)}Ar_q$. The well known equation system governing the equilibrium composition consists in the set of equations of generalized Eggert–Saha and/or mass action law type expressing partial pressures of i-th individual complex components by the help of basic ones (e, H, O, Ar) and the respective equilibrium

constants. The system is completed by the usual particle and charge balance assuming quasineutrality and equilibrium and stoichiometric conditions defining the molar amount of argon q bound to the molar amount of water before the decomposition. The calculations of this resulting nonlinear equation system were performed using our own code based on the modified Newton method. The relative precision of all resulting molar fractions was chosen better than 10^{-6}. The code converges very quickly (10–20 iterations) and is not much sensitive to the starting assessment of molar fractions of basic components. After the calculations of the composition were completed, we estimated the lowering of the ionization potential (2) which differs only slightly for different argon molar amounts q. Modified values of internal partition functions and new equilibrium constants were computed and the calculation of composition was repeated. We also examined possible influence of the Debye–Hückel pressure correction. Nevertheless at the given thermodynamic conditions the pressure correction was found to be of the order 10^{-3} which cannot influence the relations between molar fractions.

The direct comparison of our results of composition could hardly be compared with other publications which are up to our knowledge not available. Nevertheless a qualitative agreement could be established with the work of Boulos [9] who presents compositions of mixtures Ar–H_2 and Ar–O_2. Figure 1a shows how the molar fractions of electrons against temperature depend on molar amount of argon q. This was chosen from 0 to 1 with the step 0.1. The only slight changes of electron concentration are not only reason for small changes of ionization potential lowering, but also they are one of the very important elements of the reasons for using hybrid water–argon plasmas. Figure 1b shows the detail in the temperature region of 20,000 K.

Figure 2 shows the position of ionization maxima of the water–argon mixture represented by products of originating and dissolving species. It can be easily seen that the first ionization of H I, O I and Ar I occurs simultaneously whilst the second ionization of oxygen lies in the middle between the ionization peaks of Ar II and Ar III.

The equilibrium thermodynamic properties were computed according to the standard well known formulae as mass density

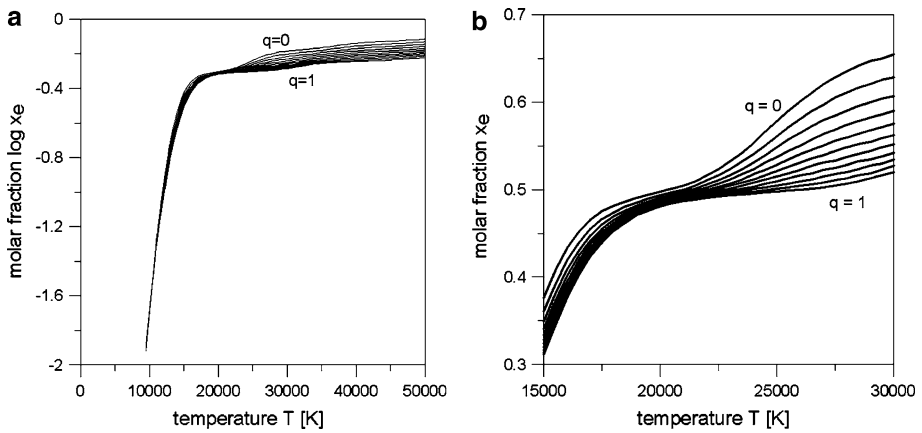

Fig. 1 (**a**) Electron concentration vs. temperature for molar amounts of argon q from 0 to 1 step 0.1, logarithmic scale. (**b**) Detailed electron concentration of Fig. 1a, linear scale

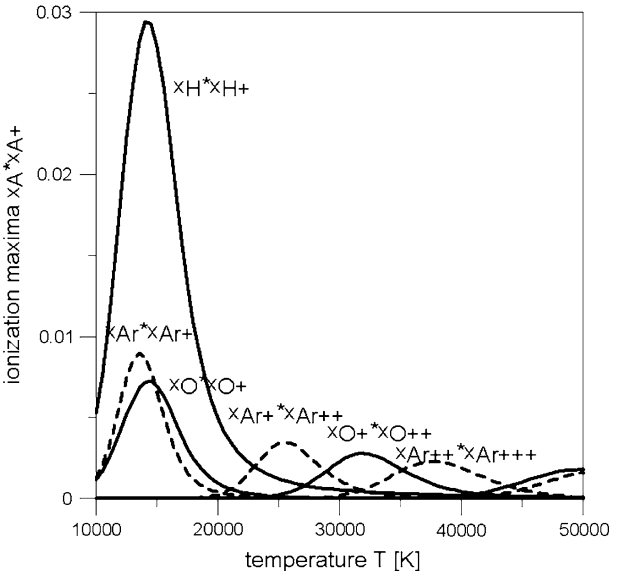

Fig. 2 Ionization maxima in the mixture 50%H_2O + 50%Ar

$$\rho = \frac{p}{RT}\sum_{i=1}^{ps} x_i M_i \tag{8}$$

enthalpy

$$H = \frac{1}{M}\sum_{i=1}^{ps} x_i H_i^0 \tag{9}$$

where $M = \sum_{i=1}^{ps} x_i\, M_i$ is the molar mass, entropy

$$S = \frac{R}{M}\sum_{i=1}^{ps} x_i\left(\frac{S_i}{R} - \ln x_i\right) \tag{10}$$

equilibrium heat capacity

$$c_p = \left(\frac{\partial H}{\partial T}\right)_p \tag{11}$$

and the equilibrium sound velocity

$$a = \sqrt{\frac{\kappa RT}{p\beta_T M}} \quad \text{with } \kappa = \frac{c_p}{c_v} \tag{12}$$

where $c_v = c_p - \frac{R}{M}\frac{(T\alpha_p)^2}{p\beta_T}$

$$\text{with } T\alpha_p = \frac{T}{v}\left(\frac{\partial v}{\partial T}\right)_p \text{ being isobaric thermal expansion and} \tag{13}$$

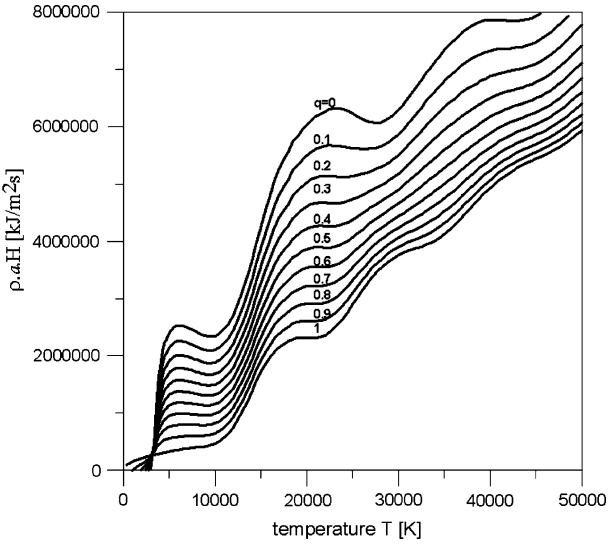

Fig. 3 Enthalpy flux ρaH vs. temperature for molar amounts of argon q from 0 to 1 step 0.1

$$p\beta_T = -\frac{p}{v}\left(\frac{\partial v}{\partial p}\right)_T \text{ isothermal compressibility.} \tag{14}$$

The necessary differentiation by temperature and pressure was performed numerically using extensive tables of composition for building up a grid of pressures around 0.1 Mpa. Having these quantities (15–19) we can calculate important constants necessary for modelling the plasma. All calculations were made for molar amounts of argon q increasing from zero to unity with step 0.1. In practice argon up to roughly $q = 0.5$ used to be added in hybrid argon–water stabilized torches. Higher amounts of argon are presented for better illustration of the processes. In Fig. 3 the product ρaH is introduced. This quantity represents the local enthalpy flux in cases when the velocity is controlled by the nozzle geometry and is near to the sound velocity. The decrease of enthalpy and also sound velocity with adding argon is sufficiently compensated by the increase of mass density. Two steep increases can be observed, first one around 3,500 K due to the dissociation processes, second between 12,000 and 16,000 K due to the first ionization. Figure 4 shows the product ρc_p which is generally needed for all types of energy balance equations. Lower values of specific heat of argon are also compensated by its higher mass densities. Moreover, we can observe differences in the ionization processes of water steam and argon. The first one takes place for water and argon together because of very similar ionization potential of hydrogen and Ar I. Towards higher temperatures the situation changes due to the higher ionization potentials of O II and O III compared to those of Ar II and Ar III.

Transport Coefficients

Method

The calculations of transport coefficients are based on the well known Enskog–Chapman method of solution of Boltzmann equation in the the 4th approximation (see e.g. [2, 4]). The solution of integral equations was developed as described by Hirschfelder et al. [8]. It

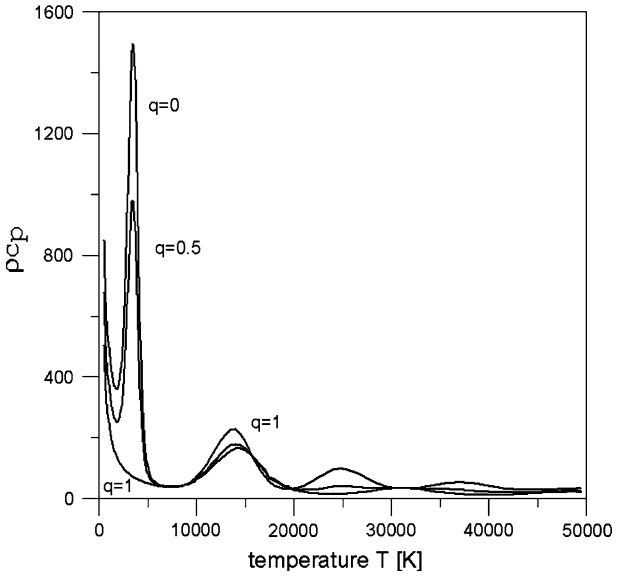

Fig. 4 The product ρc_p vs. temperature for molar amounts of argon q from 0 to 1 step 0.1

is generally known that this method is based on some important assumptions, especially that of an ideal gaseous system in the local thermodynamic equilibrium with only small perturbations caused by gradients of temperature, velocity, particle densities and external forces. These gradients and forces are causes of diffusion and thermal particle flow in the gas mixture and the transport coefficients can be regarded as proportionality coefficients between these causes and consequences. They can be defined through moments of the velocity distribution functions of mixture components.

In this way we calculated the viscosity, electrical conductivity and thermal conductivity of the H_2O + Ar mixture for molar amounts of argon q from 0 to 1 step 0.1. Let us summarize the utilized formulae:

Viscosity

$$\eta = \frac{1}{2} kT \sum_i n_i b_{i1}, \tag{15}$$

the diffusion coefficients

$$\begin{aligned} D_{ij} &= \frac{\rho p n_i}{2 n^2 m_j} \sqrt{\frac{2kT}{m_i}} c_{i1}^{ji} \\ D_i^T &= \frac{n_i m_i}{2} \sqrt{\frac{2kT}{m_i}} a_{i1} \end{aligned} \tag{16}$$

electrical conductivity

$$\sigma = \frac{e^2 n^2}{p \rho^2} \sum_i z_i \sum_j n_j m_j^2 D_{ij} \left(\sum_k n_k z_k - \frac{\rho z_j}{m_j} \right) \tag{17}$$

translational thermal conductivity (including the electron component)

$$\lambda' = -\frac{5}{4}k\sum_j n_j\sqrt{\frac{2kT}{m_j}}a_{j2} \tag{18}$$

and the thermal diffusion component

$$\lambda_t = \frac{5}{4}pk\sum_j n_j\sqrt{\frac{2kT}{m_j}}\sum_k \mathcal{D}_{jk}^{-1}\mathcal{D}_k^T c_{j1}^{kj} \tag{19}$$

with $\mathcal{D}_{ij} = \frac{n^2 m_j}{n_i\rho}D_{ij}$ and $\mathcal{D}_i^T = \frac{1}{n_i m_i}D_i$.

The coefficients a_{im}, b_{im}, c_{im}^{ji} are solutions of equation systems

$$\begin{aligned}
&\sum_{j=1}^{ps}\sum_{m=1}^{\zeta}\left(Q_{ij}^{(m,m')} - \frac{n_j}{n_i}\sqrt{\frac{m_j}{m_i}}Q_{ii}^{(m,m')}\delta_{0m}\delta_{0m'}\right)a_{jm} = \frac{15}{4}\delta_{1m}n_i\sqrt{\frac{2kT}{m_i}}\\
&\sum_{j=1}^{ps}\sum_{m=1}^{\zeta}Q_{ij}^{(m,m')}b_{jm} = -5n_i\\
&\sum_{j=1}^{ps}\sum_{m=1}^{\zeta}\left(Q_{ij}^{(m,m')} - \frac{n_j}{n_i}\sqrt{\frac{m_j}{m_i}}Q_{ii}^{(m,m')}\delta_{0m}\delta_{0m'}\right)c_{jm}^{hk} = (\delta_{ih}-\delta_{ik})\delta_{0m}\frac{3}{\sqrt{2m_i kT}}
\end{aligned} \tag{20}$$

with

$$Q_{ij}^{(m,m')} = \sum_{k=1}^{ps} n_i n_k\left[\delta_{ij}(M_{mm'}^l)_{ik} + \delta_{jk}(N_{mm'}^l)_{ik}\right] \tag{21}$$

where $M_{mm'}^l$ and $N_{mm'}^l$ are the matrix elements of the linearized Boltzmann collision operator expressed by the collision integrals

$$\begin{aligned}
(M_{mm'}^l)_{ik} &= 8\sum_{s,r} V_{lmm'}^{(s,r)}\mu_i^a\mu_k^b(\mu_i-\mu_k)^c\Omega_{ik}^{(s,r)}\\
(N_{mm'}^l)_{ik} &= 8\sum_{s,r} W_{lmm'}^{(s,r)}\mu_i^m\mu_k^{m'}\sqrt{\mu_i\mu_k}\Omega_{ik}^{(s,r)}.
\end{aligned} \tag{22}$$

where $\mu_k = \frac{m_k}{m_k+m_i}$.

The coefficients $V_{mm'}^l$, $W_{mm'}^l$ together with powers a, b, c have been tabelled sufficiently to cover needs of higher approximations.

The equation systems (24) were solved both via the inversion of matrices and using modified Gaussian procedure. As the matrices are large (for our mixture with 35 components generally 140 × 140 for the 4th approximation) and the elements may differ by many orders, it is necessary to check carefully for correct solutions.

The total thermal conductivity is then given by the sum

$$\lambda = \lambda' + \lambda_t + \lambda_{int} + \lambda_{re}$$

Where the internal thermal conductivity λ_{int} (the Eucken correction for internal degrees of freedom)

$$\lambda_{\text{int}} = \frac{2k^{3/2}}{3R\sqrt{\pi}} \sum_{i=1}^{ps} \frac{x_i(c_{pi} - 2.5R)}{\sum_{j=1}^{ps} x_j q_{ij} \sqrt{\frac{2m_i m_j}{m_i + m_j}}} \tag{23}$$

and the reaction thermal conductivity

$$\lambda_{\text{re}} = \frac{2k^{3/2}}{3R^2\sqrt{\pi}T^{3/2}} \sum_{i=5}^{ps} (\mathrm{d}t_i Hr_i) \tag{24}$$

Where Hr_i means the enthalpy of reaction constituting the i-th complex component from the (first four) basic ones at given temperature and

$$\mathbf{dt} = \mathbf{Rm}^{-1} * \mathbf{Hr}$$

with

$$Rm_{kl} = \sum_{i=1}^{ps-1} \sum_{j=i+1}^{ps} \frac{(sk_{ki}x_j - sk_{kj}x_i)(sk_{li}x_j - sk_{lj}x_i)}{x_i x_j} q_{kl} \sqrt{\frac{2m_i m_j}{m_i + m_j}}.$$

Here in both Eqs. 27 and 28 q_{ij} denotes the effective collision cross section.

Collision Integrals

For the collision integrals $\Omega_{ij}^{(s,r)}$ we use the classical definition presented by Hirschfelder et al. [8]. Generally we have to deal with four main interaction types: Coulomb interactions, Lennard–Jones interactions, electron–neutral interactions and ion–neutral interactions.

For the mutual interactions of charged particles the repulsive and attractive Coulomb potentials screened at the Debye shielding length were used. The collision integrals were calculated by Mason et al. [10] and completed by Devoto [11]. As their results are enough only up to 3rd approximation, we calculated the for the 4th approximation missing necessary integrals $(T^*)^2\Omega^{(s,r)*}$ for $(s, r) = (1, 6), (1, 7), (2, 5), (2, 6), (3, 4), (3, 5), (4, 4)$. They are presented in Table 1.

For the calculation of real collision integrals

$$\Omega_{ij}^{(s,r)} = \pi r_{ij}^2 \sqrt{\frac{kT}{2\pi\mu_{ij}}} \Omega^{(s,r)*}(T^*) \tag{25}$$

with $r_{ij} = \sqrt{\frac{\varepsilon_0 kT}{e^2 \sum_i n_i z_i^2}}$ and $T_{ij}^* = \frac{4\pi\varepsilon_0}{e^2} \frac{kTr_{ij}}{abs(z_i z_j)}$

we abandoned the coefficients A^*, B^*, C^* and E^*, F^*, G^* presented in [8, 10] and calculated the values of respective integrals $(T^*)^2\Omega^{(s,r)*}$ directly. Then we used the analytical approximation

$$(T^*)^2\Omega^{(s,r)*} = \exp[A + B\log T^* + C(\log T^2) + D(\log T^3)]. \tag{26}$$

in two intervals of energy $T^* \leq 1$ and $T^* \geq 1$ because the whole interval $0.1 \leq T^* \leq 10{,}000$ is too large to be covered with satisfactory precision.

For the interactions of neutral particles the Lennard–Jones (6–12) potential was used. The values of σ_{LJ} and $(\varepsilon/k)_{LJ}$ available were taken from [12], the values for O_3, HO_2, H_2O_2

Table 1 Collision integrals of both the attractive and repulsive screened Coulomb potentials necessary for the 4th approximation

T*	$T^{*2}\Omega^{(1,6)}a$	$T^{*2}\Omega^{(1,6)}r$	$T^{*2}\Omega^{(1,7)}a$	$T^{*2}\Omega^{(1,7)}r$	$T^{*2}\Omega^{(2,5)}a$	$T^{*2}\Omega^{(2,5)}r$	$T^{*2}\Omega^{(2,6)}a$	$T^{*2}\Omega^{(2,6)}r$	$T^{*2}\Omega^{(3,4)}a$	$T^{*2}\Omega^{(3,4)}r$	$T^{*2}\Omega^{(3,5)}a$	$T^{*2}\Omega^{(3,5)}r$	$T^{*2}\Omega^{(4,4)}a$	$T^{*2}\Omega^{(4,4)}r$
0.1	0.01856	0.00800	0.01547	0.00701	0.02537	0.01793	0.02276	0.01570	0.03449	0.01833	0.02844	0.01580	0.03310	0.02545
0.2	0.02798	0.01522	0.02283	0.01303	0.05468	0.03725	0.04643	0.03181	0.06378	0.03945	0.05142	0.03311	0.07733	0.05615
0.3	0.03422	0.02107	0.02767	0.01779	0.07756	0.05435	0.06412	0.04569	0.08841	0.05898	0.07032	0.04864	0.11616	0.08519
0.4	0.03895	0.02595	0.03132	0.02171	0.09595	0.06943	0.07806	0.05770	0.10962	0.07676	0.08625	0.06248	0.14982	0.11203
0.6	0.04601	0.03375	0.03675	0.02787	0.12441	0.09491	0.09935	0.07762	0.14462	0.10783	0.11196	0.08613	0.20575	0.15960
0.8	0.05128	0.03985	0.04079	0.03262	0.14611	0.11584	0.11542	0.09368	0.17277	0.13421	0.13223	0.10578	0.25109	0.20055
1	0.05550	0.04484	0.04403	0.03648	0.16369	0.13354	0.12836	0.10710	0.19630	0.15707	0.14894	0.12254	0.28920	0.23637
2	0.06930	0.06129	0.05455	0.04903	0.22161	0.19508	0.17067	0.15283	0.27704	0.23980	0.20528	0.18160	0.42138	0.36805
3	0.07778	0.07129	0.06099	0.05657	0.25733	0.23429	0.19659	0.18144	0.32844	0.29467	0.24059	0.21975	0.50632	0.45671
4	0.08394	0.07844	0.06566	0.06194	0.28332	0.26296	0.21539	0.20219	0.36629	0.33561	0.26641	0.24784	0.56913	0.52337
6	0.09280	0.08852	0.07236	0.06950	0.32069	0.30407	0.24237	0.23177	0.42116	0.39521	0.30365	0.28832	0.66044	0.62104
8	0.09920	0.09565	0.07719	0.07483	0.34765	0.33350	0.26179	0.25285	0.46096	0.43838	0.33055	0.31741	0.72679	0.69214
10	0.10420	0.10116	0.08097	0.07895	0.36877	0.35638	0.27698	0.26922	0.49224	0.47216	0.35164	0.34009	0.77897	0.74796
20	0.11997	0.11813	0.09284	0.09164	0.43533	0.42744	0.32479	0.31993	0.59113	0.57784	0.41812	0.41068	0.94413	0.92324
30	0.12930	0.12795	0.09986	0.09898	0.47477	0.46885	0.35308	0.34945	0.64987	0.63971	0.45750	0.45189	1.04231	1.02621
40	0.13596	0.13488	0.10486	0.10416	0.50294	0.49813	0.37326	0.37033	0.69183	0.68352	0.48560	0.48103	1.11249	1.09924
60	0.14536	0.14459	0.11193	0.11142	0.54283	0.53929	0.40182	0.39968	0.75128	0.74508	0.52536	0.52199	1.21196	1.20203
80	0.15205	0.15144	0.11695	0.11655	0.57124	0.56841	0.42216	0.42046	0.79362	0.78862	0.55365	0.55095	1.28286	1.27482
100	0.15724	0.15673	0.12084	0.12051	0.59334	0.59097	0.43797	0.43655	0.82653	0.82232	0.57563	0.57336	1.33800	1.33121
200	0.17335	0.17307	0.13291	0.13273	0.66223	0.66089	0.48725	0.48646	0.92900	0.92657	0.64401	0.64272	1.50988	1.50593
300	0.18273	0.18254	0.13994	0.13981	0.70267	0.70172	0.51617	0.51561	0.98904	0.98730	0.68405	0.68314	1.61067	1.60784
400	0.18936	0.18922	0.14490	0.14481	0.73141	0.73067	0.53671	0.53628	1.03166	1.03030	0.71247	0.71176	1.68221	1.68000
600	0.19865	0.19856	0.15184	0.15179	0.77195	0.77144	0.56567	0.56539	1.09174	1.09079	0.75253	0.75205	1.78302	1.78148
800	0.20520	0.20513	0.15673	0.15669	0.80071	0.80034	0.58621	0.58601	1.13438	1.13366	0.78097	0.78061	1.85448	1.85331
1000	0.21024	0.21019	0.16050	0.16047	0.82300	0.82271	0.60212	0.60197	1.16746	1.16690	0.80303	0.80275	1.90986	1.90893
10000	0.25966	0.25978	0.19726	0.19737	1.04724	1.04765	0.76130	0.76166	1.50703	1.50750	1.02880	1.02921	2.47675	2.47753

Table 2 Lennard-Jones (6–12) parameters for neutral species

	σ_{LJ} [Å]	$(\varepsilon/k)_{LJ}$
H	2.708	37
O	3.050	106.7
Ar	3.432	122.4
H_2	2.915	38
O_2	3.433	113
O_3	3.8	107
OH	3.15	80
HO_2	3	100
H_2O	2.64	809
H_2O_2	3	100

which have only minor importance in the mixture were roughly estimated by the help of usual combination rules (see Table 2).

In our previous work [13] we calculated all the collision integrals $\Omega_{ij}^{(s,r)}$ necessary for the 4th approximation by ourselves. Then we used the analytical fitting formula in the form

$$\Omega^{(s,r)*} = \frac{A^{(s)*}}{(r+1)T^*} + \frac{B^{(s)*}\Gamma(r+\frac{3}{2})}{\sqrt{T^*}(r+1)!} + C^{(s)*} + D^{(s)*}\sqrt{T^*}\frac{\Gamma(r+\frac{5}{2})}{(r+1)!} \tag{27}$$

For the electron–neutral interaction H, O, H_2O, O_2, H_2 and OH the momentum transfer cross sections recommended by Spencer and Phelps [14] have been used. We derived the necessary higher order cross sections up to $l = 4$ using the rule of rigid sphere model

$$q^{(s)} = \left(1 - \frac{1 + (-1)^s}{2(s+1)}\right) q^{(1)} \tag{28}$$

and then we calculated the collision integrals by direct integration of available data

$$\Omega^{(s,r)} = \sqrt{\frac{kT}{2\pi\mu}} \int_0^\infty e^{-\gamma^2} \gamma^{2r+3} q^{(s)}(g) \mathrm{d}\gamma. \tag{29}$$

The effective elastic collision cross sections for ion–neutral interactions are based on the polarizabilities ξ which were taken for H, O, H_2O, O_2, H_2 and OH from Svehla [15] (Table 3).

Table 3 Polarizabilities of water decomposition products [15]

	ξ [Å^3]
H	0.83
O	0.59
H_2	0.79
O_2	1.60
OH	1.42
H_2O	1.65

Here

$$q^{(s)} = 2\pi\sqrt{\frac{4d}{\frac{1}{2}\mu g^2}}A^{(s)} \quad \text{where } d = \frac{z^2e^2\xi}{2\varepsilon_0} \tag{30}$$

ξ [A^3] being the polarizability of neutral particle. According to the definition, the collision integral is then

$$\Omega^{(s,r)} = \pi\sqrt{\frac{z^2e^2\xi}{\varepsilon_0\mu}}\Gamma\left(r+\frac{3}{2}\right)A^{(s)} \tag{31}$$

where $A^{(1)} = 0.29629$, $A^{(2)} = 0.30846$, $A^{(3)} = 0.41172$, $A^{(4)} = 0.42225$.

For argon species we used the already calculated collision integrals for Ar-Ar+ from Devoto [11]. Of course, for more complex species (O_3, HO_2, H_2O_2) occurring at lower temperatures where no detailed cross section data are available the rigid sphere model was applied with diameters already introduced in Table 2. In this temperature region both the occurrence of these species and the degree of ionization are low and therefore the influence of such ion–atom collisions on transport coefficients is negligible.

Results for the Mixture $(H_2O)_{(1-q)}Ar_q$

Figures 5–7 show the viscosity, electrical conductivity, and total thermal conductivity of the mixture $(H_2O)_{(1-q)}Ar_q$ calculated in the temperature region 400–50,000 K and at the pressure 0.1 Mpa. The molar amount of argon varies from 0 (pure water steam) to 1 (pure argon) step 0.1 as in previous sections.

As one can observed in Fig. 5 the increase of viscosity of the mixture with addition of argon is at temperatures up to 20,000 K controlled by its molar amount proportionally

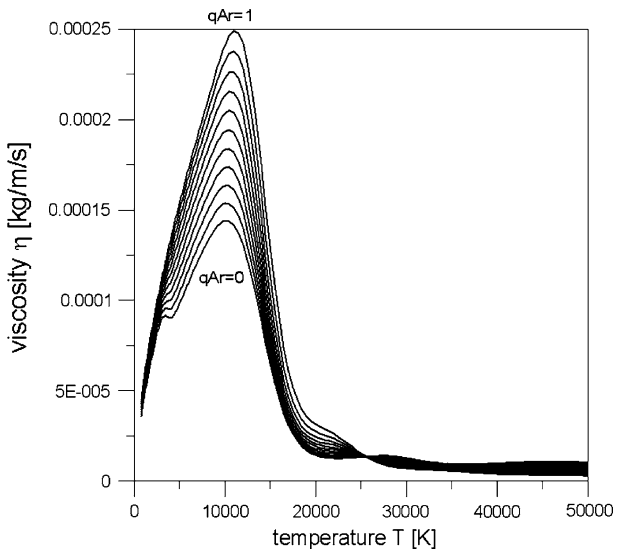

Fig. 5 Viscosity of the $(H_2O)_{(1-q)}Ar_q$ mixture

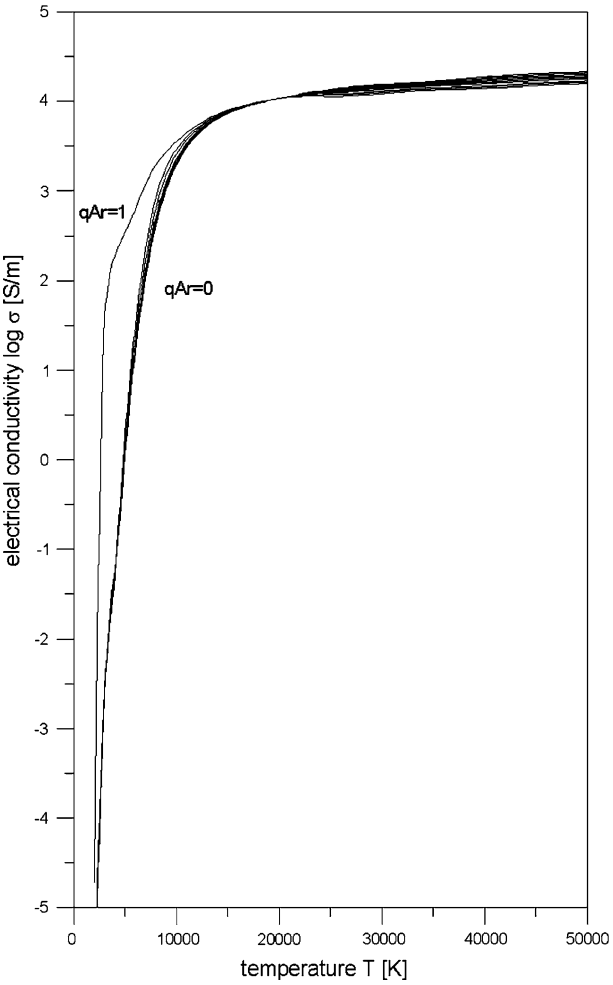

Fig. 6 Electrical conductivity of the $(H_2O)_{(1-q)}Ar_q$ mixture

because of its high mass. At higher temperatures the differences are much smaller because the mixture is already nearly fully ionized and interactions of charged particles prevail. The picture depends on changes of leading ionization maxima.

Figure 6 presents an interesting effect of strong influence of even small amount of H_2O mixed with argon on its electrical conductivity at temperatures below 10,000 K. It can be explained by the fact that the e–Ar cross section is in this energy region more than 10 times smaller compared with that of e–H and also considerably smaller compared with that of e–O. Very similar effect was described on the electrical conductivity of the mixture Ar–H_2–Cu which have been studied by Cressault and Gleizes [16].

In Fig. 7 we can see a rather smooth and regular behavior of the translational thermal conductivity, which is only disturbed by two strong maxima of the reaction component, first coming from dissociations, second from ionizations. The elevation of the dissociation maximum is perfectly inversely proportional to the amount of argon, which is obvious. The height of the dissociation maximum changes with the argon amount in a more complex

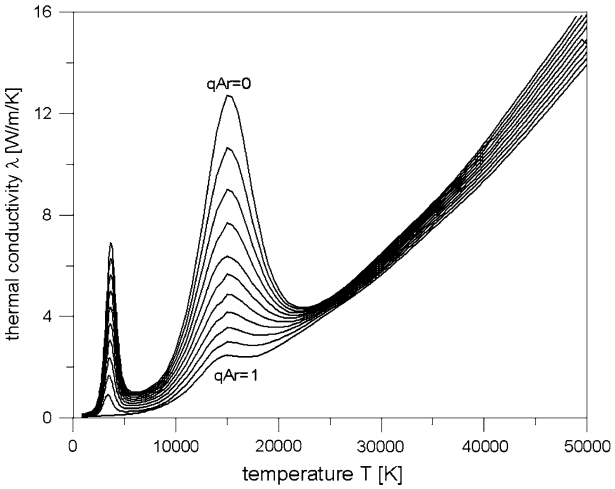

Fig. 7 Thermal conductivity of the $(H_2O)_{(1-q)}Ar_q$ mixture

way because the reaction component of thermal conductivity depends not only on reaction enthalpies which are in the case of first ionization similar as those of oxygen and hydrogen but it is also inversely proportional to the square root of the mass. This is main reason for the peak of reaction thermal conductivity in ionizing argon being much smaller than that of oxygen and, of course, hydrogen.

Conclusions

As mentioned in the introduction our studies of thermophysical properties of the system $(H_2O)_{(1-q)}Ar_q$ are motivated by the use of hybrid water–argon plasma torch developed and used in our laboratory. Up to our knowledge both this gas mixture and pure water steam plasma have not yet been studied extensively by other authors. Of course, the results for transport coefficients of pure argon can be compared with works of many other authors (see e.g. [9, 10, 11, 16]). They are in satisfactory agreement with them taking into account strong dependence on the calculation method and type of approximation used and on effective cross sections applied. There is a number of publications dealing with Ar–H_2 and Ar–O_2 mixtures (see e.g. [9, 16, 17]). They present good agreement as to the general features of mixing rules and of the special importance of an admixture of a small amount of species with low value of the electron–atom cross section on the electrical conductivity of pure argon. In the region of higher temperatures where only monatomic species occur it is possible to regard very roughly the water steam being a mixture of 2/3 of hydrogen components and 1/3 of oxygen components the respective electron gas being subdivided between both hydrogen and oxygen. In such a way the comparison is possible and taking e.g. the $H_2$and O_2 tables from [9] we can do rough comparison. The agreement has been found, similarly as in case of pure argon, also satisfactory.

Our results not only try to fill in the gap of missing data and in this way to enable the necessary modelling of the water–argon torch, but also they may contribute to the question of validity of simplified mixing rules, which are used in some laboratories because of complexity of full calculations on one side and insufficient reliability and precision of

atomic and molecular data on the other. We could easily confirm the possibility of developing suitable mixing rules for both viscosity and thermal conductivity. We showed that the behavior of electrical conductivity of argon where even a small addition of H_2O has strong influence on electrical conductivity at temperatures below 10,000 K is similar as for the Ar–H_2 and Ar–O_2 mixtures from similar reasons.

Generally, as argon proved to be very interesting and efficient species for adding to the working media of water plasma torches to deploy the obvious technological advantages (see e.g. [1]), the detailed calculations of thermophysical properties showed that main reason for its utilizability has been the matter of fact that the total mass-enthalpy product remains acceptable. On the other side, the location of first ionization maximum of argon and its ionization potential are similar to that of both hydrogen and oxygen so that the electron concentration and the electrical conductivity remain practically unchanged (with the above mentioned exception) so that the electrical parameters of the water–argon plasma torches are very similar to those of pure water stabilized arcs.

Acknowledgement The author gratefully acknowledges the support of this work by the Institutional Research Plan No. AV0 Z20430508.

References

1. Hrabovsky M, Konrad M, Kopecky V, Sember V (1997) IEEE Trans Plasma Sci 25:833
2. Hrabovsky M, Krenek P (1993) Proceedings of the 11th international symposium on plasma chemistry, Loughborough, p 315
3. Hrabovský M, Kopecký V, Sember V, Kavka T, Chumak O, Konrád M (2006) IEEE Trans Plasma Sci 34:1566
4. Krenek P, Nenicka V (1984) Acta Technica CSAV 29:420
5. Chase MW Jr (ed) (1998) NIST-JANAF thermochemical tables, 4th edn. Gaithersburg
6. Glushko VP (ed) (1978) Termodinamicheskie svoistva individualnych veshchestv, 3rd edn. Izd Nauka, Moskva
7. NIST Atomic Spectra Database. http://physics.nist.gov
8. Hirschfelder JO, Curtiss ChF, Bird RB (1954) Molecular theory of gases and liquids. Wiley, New York, London
9. Boulos MI, Fauchais P, Pfender E (1994) Thermal plasmas fundamentals and applications, vol 1. Plenum Press, New York, London
10. Mason EA, Munn RJ, Smith FJ (1967) Phys Fluids 10:1827
11. Devoto RS (1973) Phys Fluids 16:616
12. Bird RB, Stewart WE, Lightfoot EN (2002) Transport phenomena, 2nd edn. Willey, New York
13. Krenek P (1991) Acta Technica CSAV 36:560
14. Spencer FE Jr, Phelps AV (1976) Proceedings of the 15th symposium on engineering aspects MHD, Philadelphia, p IX.9.1
15. Svehla RA (1961) NASA Tech Rep R 132
16. Cressault Y, Gleizes A (2004) J Phys D: Appl Phys 37:560
17. Capitelli M, Gorse C, Longo S, Giordano D (1998) JTHT, AIAA 98:2936